Phase-contrast magnet resonance imaging reveals regional, transmural, and base-to-apex dispersion of mechanical dysfunction in patients with long QT syndrome

Johannes Brado,[*†] Markus J. Dechant, MD,[†‡] Marius Menza, PhD,[†§] Adriana Komancsek,[†§] Corinna N. Lang, MD,[*†] Heiko Bugger, MD,[*†] Daniela Foell, MD,[*†] Bernd A. Jung, PhD,[‖] Brigitte Stiller, MD,[†‡] Christoph Bode, MD,[*†] Katja E. Odening, MD[*†¶]

*From the *Department of Cardiology and Angiology I, Heart Center, University of Freiburg, Freiburg, Germany, †Faculty of Medicine, University of Freiburg, Freiburg, Germany, ‡Department of Pediatric Cardiology, Heart Center, University of Freiburg, Freiburg, Germany, §Department of Radiology and Medical Physics, Medical Center, University of Freiburg, Freiburg, Germany, ‖Department of Diagnostic and Pediatric Radiology, University Hospital of Bern, Bern, Switzerland, and ¶Institute for Experimental Cardiovascular Medicine, Heart Center, University of Freiburg, Freiburg, Germany.*

BACKGROUND Regional dispersion of prolonged repolarization is a hallmark of long QT syndrome (LQTS). We have also revealed regional heterogeneities in mechanical dysfunction in transgenic rabbit models of LQTS.

OBJECTIVE In this clinical pilot study, we investigated whether patients with LQTS exhibit dispersion of mechanical/diastolic dysfunction.

METHODS Nine pediatric patients with genotyped LQTS (12.2 ± 3.3 years) and 9 age- and sex-matched healthy controls (10.6 ± 1.5 years) were subjected to phase-contrast magnetic resonance imaging to analyze radial (Vr) and longitudinal (Vz) myocardial velocities during systole and diastole in the left ventricle (LV) base, mid, and apex. Twelve-lead electrocardiograms were recorded to assess the heart rate–corrected QT (QTc) interval.

RESULTS The QTc interval was longer in patients with LQTS than in controls (469.1 ± 39.4 ms vs 417.8 ± 24.4 ms; $P < .01$). Patients with LQTS demonstrated prolonged radial and longitudinal time-to-diastolic peak velocities (TTP), a marker for prolonged contraction duration, in the LV base, mid, and apex. The longer QTc interval positively correlated with longer time-to-diastolic peak velocities (correlation coefficient 0.63; $P < .01$). Peak diastolic velocities were reduced in LQTS in the LV mid and apex, indicating impaired diastolic relaxation. In patients with LQTS, regional (TTPmax-min) and transmural (TTPVz-Vr) dispersion of contraction duration was increased in the LV apex (TTPVz_max-min: 38.9 ± 25.5 ms vs 20.2 ± 14.7 ms; $P = .07$; TTPVz-Vr: −21.7 ± 14.5 ms vs −8.7 ± 11.3 ms; $P < .05$). The base-to-apex longitudinal relaxation sequence was reversed in patients with LQTS compared with controls (TTPVz_base-apex: 14.4 ± 14.9 ms vs −10.1 ± 12.7 ms; $P < .01$).

CONCLUSION Patients with LQTS exhibit diastolic dysfunction with reduced diastolic velocities and prolonged contraction duration. Mechanical dispersion is increased in LQTS with an increased regional and transmural dispersion of contraction duration and altered apicobasal longitudinal relaxation sequence. LQTS is an electromechanical disorder, and phase-contrast magnetic resonance imaging Heterogeneity in mechanical dysfunction enables a detailed assessment of mechanical consequences of LQTS.

KEYWORDS LQTS; Magnet resonance imaging; Diastolic dysfunction; Dispersion of contraction duration; Heterogeneity in mechanical dysfunction

(Heart Rhythm 2017;14:1388–1397) © 2017 Heart Rhythm Society. All rights reserved.

Introduction

Long QT syndrome (LQTS) is an inherited arrhythmogenic disease of variable penetrance caused by mutations in genes encoding for cardiac ion channels or channel-modifying proteins that are crucial for cardiac repolarization and whose malfunction prompts prolonged repolarization.[1] This leads to the clinically evident sign of LQTS, a prolonged QT interval, and to the risk of developing lethal ventricular arrhythmia.[2] Data published in the last decade, however, suggested that the electrophysiological substrate of arrhythmias is not only the prolongation of action potential duration (APD) itself but also an increased spatial dispersion of APD throughout the different regions of the heart.[3] Electrical and mechanical function of the heart is inevitably linked together via electromechanical and reverse

Address reprint requests and correspondence: Dr Katja E. Odening, Department of Cardiology and Angiology I, Heart Center, University of Freiburg, Hugstetter Str 55, Freiburg 79106, Germany. E-mail address: katja.odening@uniklinik-freiburg.de.

mechanoelectrical coupling.[4,5] Therefore, changes in electrical function may lead to mechanical dysfunction. The first study describing altered cardiac mechanics in patients with LQTS was published in 1991.[6] Since then, several studies could confirm the initial finding that LQTS is not purely an electrical disease, but does affect cardiac mechanics as well: Hearts from patients with LQTS showed a prolonged contraction duration[6–11] and an increased dispersion of contraction duration.[12–16] These changes in mechanical function are, however, only subtle and do not affect global cardiovascular parameters such as ejection fraction or cardiac output and do not lead to significant clinical impairment and heart failure. But the extent of mechanical dysfunction seems to correlate with the arrhythmic risk of an individual patient and may thus improve risk stratification in LQTS.[9,10,13,14,16] Most studies used echocardiography-based methods to evaluate mechanical alterations such as measurements of myocardial wall thickening in M-mode technique and wall motion velocities through tissue Doppler and myocardial strain imaging.[6–9,12–15] With magnetic resonance imaging (MRI)–based tissue phase mapping (TPM), which has evolved over the past decades, there is a promising alternative allowing a complete 3-dimensional coverage of myocardial velocities assessing radial, longitudinal, and rotational aspects with high spatial and temporal resolution. Using this technique, we could previously demonstrate a pronounced impairment of diastolic relaxation, prolonged contraction duration, and increased regional mechanical dispersion in transgenic rabbits with LQTS type 2.[16] Moreover, we could demonstrate its potential use for arrhythmic risk prediction.[10,16]

In this study, we present the most detailed analysis of left ventricular (LV) contraction duration and dispersion of contraction duration in LQTS done so far by using the full advantages of TPM MRI over echocardiography.

Methods

A more detailed method description can be found in the Supplemental Data.

Ethical aspects

The clinical study was approved by the institutional ethics committee on human research. Written informed consent was obtained from all parents or legal guardians as none of the participants had reached full age. All patients with LQTS and healthy controls were subjected to standard 12-lead electrocardiography (ECG), 24-hour Holter ECG, and MRI.

Study population

The study was conducted in pediatric patients with LQTS, since they (1) had no (implantable cardioverter-defibrillator–based) contraindications for MRI, (2) had no concomitant diseases that might confound the impact of LQTS on cardiac mechanics, and (3) were in an early asymptomatic disease stage, allowing detection of potential parameters for early risk stratification.

MRI measurements

MRI was performed on a 1.5-T MRI system (Symphony, Siemens, Germany). To assess global function and structure of the LV, standard cine cardiac MRI was performed. To assess regional systolic and diastolic myocardial velocities, TPM was carried out using ECG triggering, navigator respiration control, kt-GRAPPA–based acceleration, and black blood preparation to avoid blood flow–related artifacts (temporal resolution 12.7 ms; spatial resolution 1.4 $\times$ 1.4 mm^2).[10,16–18] Postprocessing was performed using customized software programmed in MATLAB (MathWorks Inc, Natick, MA). Myocardial velocities (longitudinal velocity, circumferential velocities, and radial velocity) (Figure 1A) and time-to-peak velocity (TTP) (Figure 1B) were determined for all 16 segments of the LV. Mechanical dispersion was calculated as differences in TTP (TTPmax-min) within each level (base, mid, and apex), differences between longitudinal and radial TTP (TTPVz-Vz) (an indicator of transmural dispersion), and differences between TTP in LV base and apex (TTPbase-apex).

Statistical analysis

Statistical analysis was performed using Prism 7 for Macintosh (Graphpad Software, Inc, La Jolla, CA). For normally distributed parameters, an unpaired t test was chosen to compare data and a Pearson test for correlation. For nonnormally distributed parameters, a Mann-Whitney U test was used and a Spearman test for correlation. Receiver operating characteristic analyses were performed to identify cutoff values. All data are presented as mean $\pm$ SD. A P value of $<.05$ was considered significant.

Results

A more detailed description of 12-lead ECG, 24-hour Holter ECG, and standard cine MRI can be found in the Supplemental Data.

Study cohort

Nine pediatric patients and 9 age- and sex-matched healthy controls (5 girls and 4 boys each; mean age: patients 12.2 $\pm$ 3.3 years vs controls 10.6 $\pm$ 1.5 years; $P = 0.1841$) were included in the study (Supplemental Table 1). Six patients were asymptomatic having been diagnosed either through incidental findings of longer heart rate–corrected QT (QTc) interval or during family screening for LQTS. Three patients were symptomatic, 1 had experienced syncope, and 2 had suffered from presyncope during exercise (Table 1). Seven patients had LQTS type 1, 1 LQTS type 2, and 1 LQTS type 5 (Table 1). All were receiving antiarrhythmic β-blocker therapy, but none had thus far experienced any documented ventricular tachycardia or (survived) sudden cardiac death.

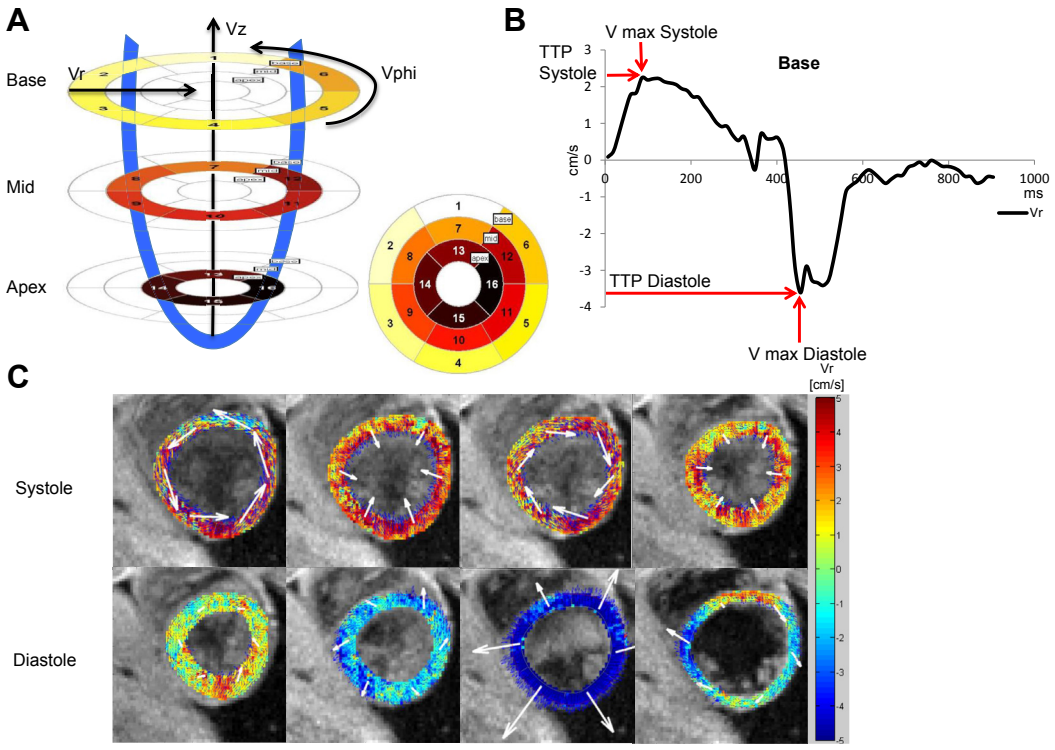

Figure 1 Phase-contrast MRI. **A:** Schematic of the left ventricle and generation of bull's-eye plots according to AHA 16-segment model. Longitudinal velocity (Vz; along the base-to-apex axis), radial velocity (Vr; toward the center), and circumferential velocities (Vphi) are indicated. **B:** Velocity-time diagram with exemplary data of basal radial motion. Positive values represent motion toward the center and negative values away from the center. Systolic and diastolic peak velocities (Vmax) and the corresponding time-to-peak velocities (TTP) are indicated. **C:** Exemplary tissue phase mapping MRI scans of the mid-left ventricle of 1 patient with LQTS. In-plane wall motion is indicated by arrows and color coded as indicated in the legend. Upper panel: motion during systole; lower panel: motion during diastole.

ECG

QT intervals and QTc intervals were longer in patients with LQTS than in healthy controls (QTc interval: patients 469.1 ± 39.4 ms vs controls 417.8 ± 24.4 ms; $P < .01$) (Supplemental Table 2 and Supplemental Figure 1).

TPM MRI

Myocardial velocities

Standard parameters of global cardiac function assessed with cine MRI were similar in patients with LQTS and controls (Supplemental Table 3). Similarly as seen with global ejection fraction, regional and segmental systolic longitudinal peak velocities were similar in patients with LQTS and controls (Supplemental Figures 2A and 2B and Table 2). Radial peak systolic velocities were reduced in the apex and apicoseptal segment of patients, but similar in all other regions and segments (Supplemental Figures 2C and 2D and Supplemental Table 4). Diastolic peak velocities were reduced in several LV regions and segments in patients with LQTS, indicating an impaired relaxation: In patients with LQTS, diastolic longitudinal velocities were significantly reduced in the LV apex and marginally in the LV mid. Moreover, diastolic longitudinal velocities were reduced in apicoseptal and apicoinferior segments (Figure 2A and 2B and Table 2). Similarly, radial diastolic peak velocities were reduced in patients with LQTS in the LV apex, whereas no differences were found in the LV base and mid. Furthermore, radial diastolic peak velocities were reduced in basal anterolateral, apicoanterior, and apicolateral segments (Figures 2C and 2D and Table 2).

Time-to-Peak Velocities

Time-to-systolic peak velocity was similar in patients with LQTS and controls in longitudinal and radial directions (Supplemental Table 4).

In contrast, time-to-diastolic peak velocity, a marker for contraction duration and delay in relaxation, was significantly longer in patients with LQTS than in controls in both longitudinal and radial directions. In the longitudinal direction, time-to-diastolic peak (TTP_Vz_dia) is longer in the LV base and mid as well as in all basal, mid, and apicoseptal segments (Figures 3A and 3B and Table 2). In the radial direction, time-to-diastolic peak (TTP_Vr_dia) was equally prolonged in the LV base, mid, and apex. On the segmental level, a longer TTP_Vr_dia could be seen in all but the inferoseptal segments (Figures 3D and 3E and Table 2).

Correlation of electrical and mechanical parameters

There was a clear positive correlation between a longer QTc interval, a marker for prolonged repolarization, and longer

Table 1 Characteristics of patients with LQTS

Patient	Age (y)	Medication	Genotype	Mutation	Symptoms (mode of diagnosis)
1	12	Metoprolol 47.5 mg once daily	LQT5	*KCNE1*-D85N (c.253G>A) heterozygous missense mutation	None (family history)
2	17	Metoprolol 47.5 mg twice daily	LQT1	*KCNQ1*-P59Rfs*228 (c.169_175dupGGCGCCC) heterozygous duplication; *KCNH2*-R1047L (c.3140G>T) heterozygous polymorphism	Presyncopes during exercise
3	10	Metoprolol 23.75 mg twice daily	LQT1	*KCNQ1*-P59Rfs*228 (c.169_175dupGGCGCCC) heterozygous duplication; *KCNH2*-R1047L (c.3140G>T) heterozygous polymorphism	None (family history; sibling to patient 2)
4	11	Metoprolol 23.75 mg twice daily	LQT1	*KCNQ1*-IVS7+5G>C (c.1032+5G>C) heterozygous splice site mutation	Syncopes
5	14	Atenolol 25 mg 1-0-½	LQT1	*KCNQ1*-M520R (c.1559T>G) heterozygous missense mutation	None (family history)
6	15	Bisoprolol 2.5 mg once daily	LQT1	*KCNQ1*-E160del (c.478_480delGAG) heterozygous in frame deletion	None (incidental ECG finding in routine sport examination)
7	7	Propranolol 10 mg twice daily	LQT1	*KCNQ1*-R231C (c.691C>T) heterozygous missense mutation	None (family history)
8	9	Propranolol 15 mg twice daily	LQT1	*KCNQ1*-V416Gfs*46 (c.1247_1248deITG) heterozygous frame shift deletion	None (incidental ECG finding in the treatment of ADHD)
9	15	Propranolol 10 mg three times daily	LQT2	*KCNH2*-S649F (c.1946C>T) heterozygous missense mutation	Presyncopes during exercise

LQT1 = long QT syndrome type 1; LQT2 = long QT syndrome type 2; LQT5 = long QT syndrome type 5; *KCNE1* = gene encoding for minK, the beta-subunit to slow delayed rectifier potassium current I_{Ks}; *KCNQ1* = gene encoding for KvLQT1, the alpha-subunit to slow delayed rectifier potassium current I_{Ks}; *KCNH2* = gene encoding for HERG, the alpha-subunit to rapid delayed rectifier potassium current I_{Kr}.

time-to-diastolic peak velocities (TTP_dia), a marker for prolonged contraction duration and delay of relaxation, in radial and longitudinal directions (Figures 3C and 3F and Table 2).

Global diastolic peak velocities showed no significant correlation with the QTc interval. In the apex, where the differences between patients and controls were most pronounced, reduced longitudinal diastolic peak velocities tended to correlate with a longer QTc interval (Supplemental Table 4).

Mechanical dispersion

To assess potential differences in mechanical dispersion, regional, apicobasal, and radial-to-longitudinal dispersion of TTP_dia was calculated.

Dispersion of TTP within all segments of 1 region (defined as the difference between maximum and minimum TTP, TTPmax-min) tended to show higher dispersion in the LV apex of patients for longitudinal velocities. In contrast, no differences in regional dispersion were found in the LV base and mid in both longitudinal and radial directions (Figures 4A and 4B and Table 2).

Dispersion between longitudinal and radial diastolic TTP (TTPVz-Vr), an indicator of transmural dispersion of relaxation, revealed regional differences in patients and controls: In the LV base, a longer TTP was observed in the longitudinal direction than in the radial direction; in the LV mid, an almost equal TTP was observed in both directions; and in the LV apex, a longer TTP was identified in the radial direction than in the longitudinal direction. This apical dispersion between longitudinal and radial diastolic TTP was significantly greater in patients with LQTS than in controls (Figures 4C–4E and Table 2).

Apicobasal dispersion of TTP (TTPbase-apex), a marker for apicobasal sequence of relaxation, demonstrated a similar sequence in patients with LQTS and controls in the radial direction with longer apical TTP than basal TTP_dia (Figures 5A and 5B and Table 2). In the longitudinal direction, controls showed the same sequential pattern of relaxation with longer apical TTP. In contrast, patients with LQTS showed a reverse sequence with a longer basal TTP, indicating an altered sequence of base-to-apex relaxation (Figures 5C–5F and Table 2). In 8 of 9 patients with LQTS, this reverse relaxation sequence was seen (TTPVz_base-apex $\geq$0), while in 8 of 9 controls, there was either an apicobasal relaxation sequence or no apicobasal difference (TTPVz_base-apex $\leq$0).

Differentiation between patients and controls based on mechanical data

Mechanical parameters TTPVz_base-apex (area under the curve [AUC] 0.9), TTPVz-Vr in the LV base (AUC 0.83 each), and TTPVz-Vr in the LV mid (AUC 0.82 each) provided the best discrimination between patients and controls (Table 2 and Supplemental Table 4): In receiver operating characteristic analysis, TTPVz_base-apex identified patients with a cutoff of $\geq$6.4, with a sensitivity of 78%

Table 2 Main findings of TPM MRI

Variable	Patients	Controls	*P*
Vz_dia (cm/s)			
Base	−13.00 ± 2.05	−13.92 ± 2.05	0.3551
Mid	−8.87 ± 2.27	−10.72 ± 1.50	.0578
Apex	−3.73 ± 1.08	−5.39 ± 1.74	.0284*
Vr_dia (cm/s)			
Base	−5.12 ± 0.71	−4.95 ± 0.75	0.6229
Mid	−5.70 ± 0.80	−5.52 ± 0.73	0.6240
Apex	−4.76 ± 0.90	−5.89 ± 1.06	.0270*
TTP_Vz_dia (ms)			
Base	424.2 ± 41.1	376.7 ± 20.9	.0071**
Mid	424.2 ± 38.0	390.0 ± 24.7	.0167*
Apex	409.8 ± 45.5	386.8 ± 21.5	0.1899
TTP_Vr_dia (ms)			
Base	408.4 ± 42.2	362.2 ± 22.5	.0106*
Mid	428.6 ± 39.6	385.3 ± 27.2	.0157*
Apex	431.4 ± 36.7	395.5 ± 20.9	.021*
Delta_TTP_Vz_dia max-min (ms)			
Base	13.0 ± 0.2	10.0 ± 10.7	0.4228
Mid	13.0 ± 9.2	15.8 ± 8.5	0.5014
Apex	38.9 ± 25.5	20.2 ± 14.7	.0737
Delta_TTP_Vr_dia max-min (ms)			
Base	57.5 ± 19.3	59.0 ± 32.1	0.9092
Mid	27.4 ± 8.1	34.7 ± 11.2	0.1347
Apex	7.3 ± 9.5	7.2 ± 9.3	0.9804
Delta_TTP_Vz_dia_base-apex (ms)	14.4 ± 15.0	−10.1 ± 12.7	.0017**
Delta_TTP_Vr_dia_base-apex (ms)	−23.1 ± 14.3	−33.2 ± 6.7	.07
Delta_TTP_Vz-Vr_dia (ms)			
Base	15.8 ± 5.7	14.5 ± 4.5	0.5805
Mid	−4.4 ± 6.5	−1.4 ± 7.8	0.3924
Apex	−21.7 ± 14.5	−8.7 ± 11.3	.0499*

Receiver operating characteristic analyses

Variable	Cutoff (ms)	Sensitivity (%)	Specificity (%)	AUC	*P*	95% confidence interval
QTc interval	≥436	78	78	0.86	.0092**	0.70–1.00
TTP_dia_Vz_base-apex	≥6.4	78	89	0.90	.0041**	0.76–1.00
delta_TTP_Vz_dia_base-apex	≥−6.3	89	67	0.90	.0041**	0.76–1.00
TTP_Vz base	≥380	89	67	0.83	.0193*	0.63–1.00
TTP_Vr base	≥367	89	67	0.83	.0193*	0.63–1.00

Pearson correlation

Variable	*r*	*P*
QTc interval/TTP_dia_Vz	0.63	.005**
QTc interval/TTP_dia_Vr	0.598	.0088**

Vz_dia = peak diastolic longitudinal velocity; Vr_dia = peak diastolic radial velocity; TTP_Vz_dia = time-to-diastolic peak velocity in longitudinal direction; TTP_Vr_dia = time-to-diastolic peak velocity in longitudinal direction; Delta_TTP_Vz_dia (max-min) = dispersion (maximum-minimum) of longitudinal time-to-diastolic peak velocity; Delta_TTP_Vr_dia (max-min) = dispersion (maximum-minimum) of radial time-to-diastolic peak velocity; Delta_TTP_Vz_dia_base-apex = apico-basal dispersion of longitudinal time-to-diastolic peak velocity; Delta_TTP_Vr_dia_base-apex = apico-basal dispersion of radial time-to-diastolic peak velocity; Delta_TTP_Vz-Vr_dia = transmural dispersion of time-to-diastolic peak velocity; ROC-Analyses = Receiver operating characteristic analyses; AUC = area under the curve.
*p<0.05.
**p<0.01.

and a specificity of 89% (AUC 0.90; 95% confidence interval [CI] 0.76–1.00; $P < .004$); TTPVz in the base identified patients with a cutoff of ≥380 ms, with a sensitivity of 89% and a specificity of 67% (AUC 0.83; 95% CI 0.63–1.00; $P < .02$), and TTPVr in the base identified patients with a cutoff of ≥367 ms, with a sensitivity of 89% and a specificity of 67% (AUC 0.83; 95% CI 0.63–1.00; $P < .02$).

Discussion

By using TPM MRI for a detailed analysis of regional LV wall motion during contraction and relaxation, we revealed distinct alterations of diastolic peak velocities, prolongation of contraction duration, increased dispersion of contraction duration, and altered relaxation pattern in pediatric patients with LQTS compared with healthy controls. These findings expand our knowledge about mechanical dysfunction by

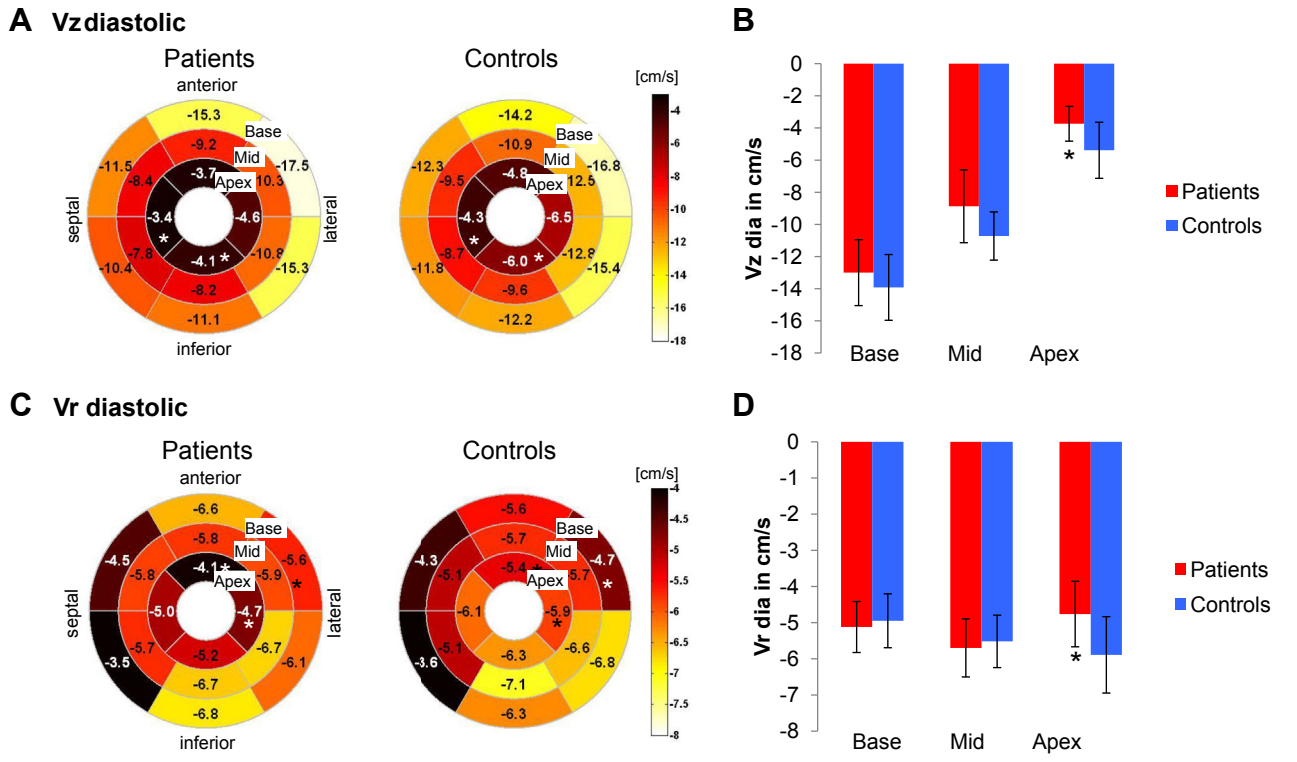

Figure 2 Diastolic velocities. **A:** Bull's-eye plots of longitudinal peak diastolic velocities (Vz diastolic in cm/s) in patients with LQTS and healthy controls (n=9 each). Vz are color coded as indicated in the legend. **B:** Bar graphs of longitudinal peak diastolic velocities averaged for the base, mid, and apex. **C:** Bull's-eye plots of radial peak diastolic velocities (Vr in cm/s) in patients with LQTS and controls. **D:** Bar graphs of radial peak diastolic velocities averaged for the base, mid, and apex. *$P < .05$.

providing novel insights into mechanical dispersion and confirm previously published studies on diastolic alterations and prolonged contraction duration[8–15,19,20]: We identified an increased regional "in-plane" and transmural dispersion of contraction duration (in the LV apex) in patients with LQTS and, most importantly, revealed a reverse gradient of apicobasal dispersion of longitudinal relaxation with prolonged contraction duration in the LV base than in the LV apex in LQTS. To our knowledge, such a detailed analysis of LV mechanical dispersion has never been done before. All these data support the notion that LQTS is an "electromechanical" rather than "pure electrical" disease.

Diastolic dysfunction in LQTS: Myocardial velocities

Several experimental and clinical studies have described a pronounced impairment of diastolic relaxation in case of prolonged repolarization: In a case report of a 2-month-old boy with extreme QT prolongation, an abnormal diastolic function was observed.[19] Similarly, Leren et al[15] identified relevant diastolic dysfunction in 25% of their patients with LQTS. In a recent study in transgenic rabbits with LQTS type 2, we demonstrated a correlation between the extent of APD prolongation and the reduction of diastolic peak velocities.[16] In the present study, diastolic impairment with reduced longitudinal and radial diastolic peak velocities was observed even in young, mainly asymptomatic patients with LQTS—particularly in the apex. As this is a region that can be difficult to assess by strain echocardiography, TPM MRI–based assessment of diastolic dysfunction may add important additional insights into diastolic dysfunction in LQTS.

Diastolic dysfunction: Prolonged contraction duration in LQTS

Through electromechanical coupling, prolonged cardiac repolarization should theoretically result in prolonged contraction duration. Our findings of pronounced prolongation of time-to-diastolic-peak velocities and prolonged time-to-peak ejection and peak filling in addition to evidence of prolonged contraction duration laid out by other clinical and experimental LQTS studies provide strong evidence for this close connection. Moreover, we could demonstrate that in LQTS the extent of electrical dysfunction (eg, longer QTc interval) correlated with the extent of prolongation of contraction duration (eg, longer diastolic TTP). The connecting mechanism is thought to be an increased Ca^{2+} influx during the prolonged plateau phase of the action potential, leading to an increased Ca^{2+} storage in the sarcoplasmic reticulum and increased Ca^{2+}-induced Ca^{2+}-release from the sarcoplasmic reticulum.[20] This hypothesis is supported by the observation made by De Ferrari et al already in 1994,[7] that Ca^{2+}-channel blockade by verapamil may abolish wall motion abnormalities and slowing of contraction in patients with LQTS.

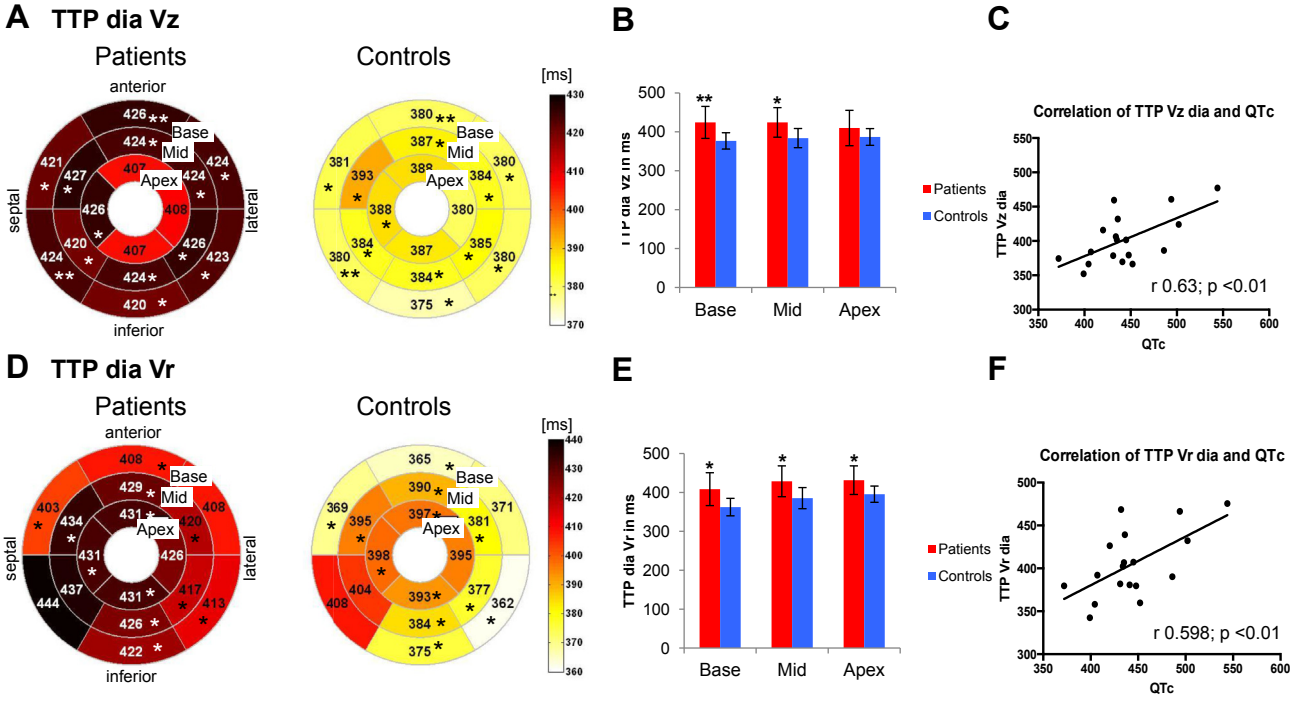

Figure 3 Time-to-diastolic peak velocities (TTP_dia) as an indicator of contraction duration. **A:** Bull's-eye plots of diastolic longitudinal time to peak (TTP_dia_Vz in ms) in patients with LQTS and healthy controls (n = 9 each). TTP_Vz are color coded as indicated in the legend. **B:** Bar graphs of diastolic longitudinal time to peak (TTP_dia_Vz) averaged for the base, mid, and apex. **C:** Bull's-eye plots of diastolic radial time to peak (TTP_dia_Vr in ms) in patients with LQTS and healthy controls. **D:** Bar graphs of diastolic radial time to peak (TTP_dia_Vr) averaged for the base, mid, and apex. **E:** Diagram indicating correlation between TTP_dia_Vz and QTc interval (CC 0.63; $P < .01$). Scale in milliseconds. **F:** Diagram indicating correlation between TTP_dia_Vr and QTc interval (CC 0.598; $P < .01$). Scale in milliseconds. *$P < .05$; **$P < .01$.

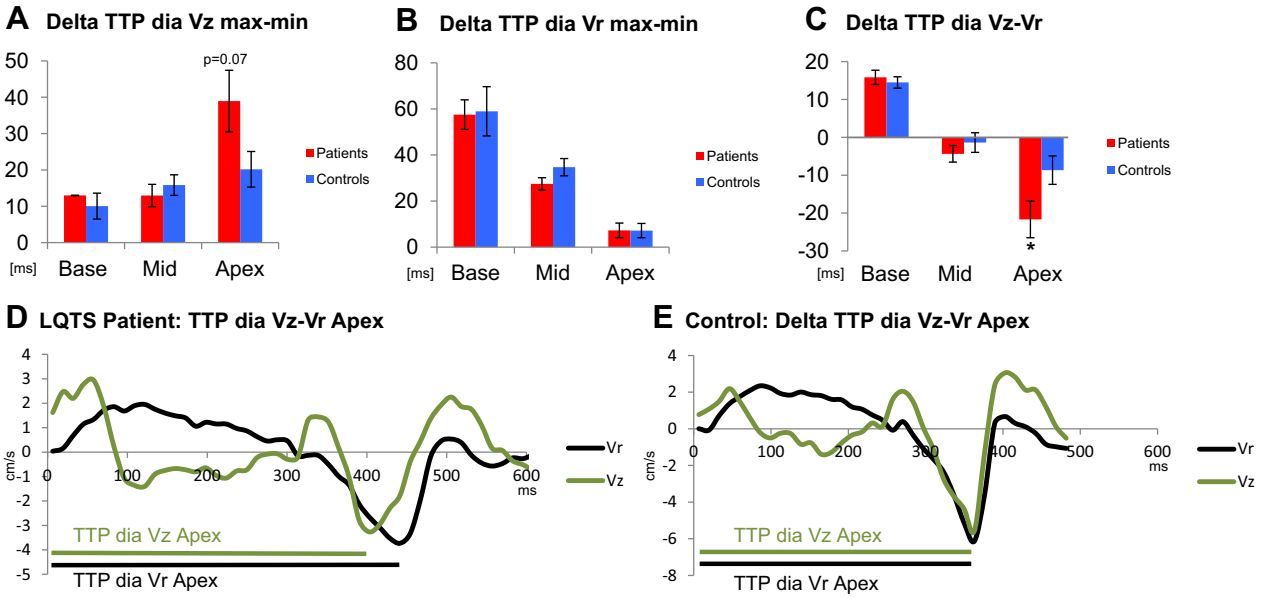

Figure 4 Dispersion of TTP. **A:** Bar graph of dispersion of longitudinal diastolic TTP in the base, mid, and apex calculated as delta TTP_Vz_dia max-min in milliseconds. **B:** Bar graph of dispersion of radial diastolic TTP in the base, mid, and apex calculated as delta TTP_Vr_dia max-min in milliseconds. **C:** Bar graph of dispersion between longitudinal and radial diastolic TTP (delta_TTPVz-Vr_dia in ms) in the base, mid, and apex as an indicator of transmural dispersion of contraction duration. Note the increased dispersion in the apex of patients. **D:** Representative velocity-time diagram of 1 patient with LQTS with apical longitudinal and radial velocities. Note the differences in time-to-diastolic peak between both velocities, representing mechanical transmural dispersion. **E:** Representative velocity-time diagram of 1 healthy control with apical longitudinal and radial velocities. Note the absence of mechanical transmural dispersion.

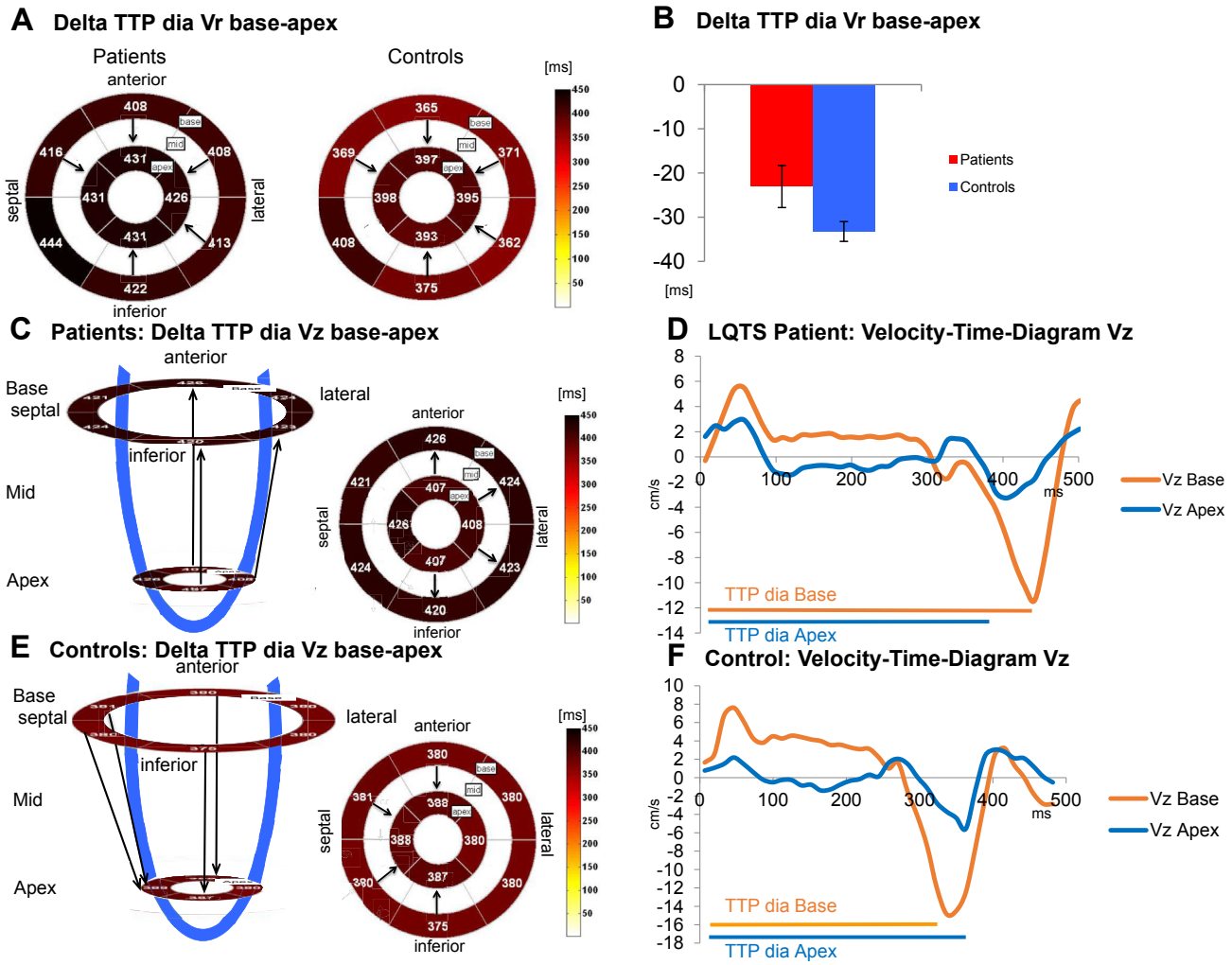

Figure 5 Apicobasal TTP_dia dispersion. **A:** Bull's-eye plots of radial diastolic TTP in the base and apex (TTP_Vr_dia in ms) in patients with LQTS and controls. **B:** Bar graphs of apicobasal dispersion of radial diastolic TTP (delta TTP_Vr_dia base-apex in ms). **C:** Schematic and bull's-eye plots of longitudinal diastolic TTP in the base and apex (TTP_Vz_dia in ms) in patients with LQTS. Note the reverse pattern (arrows) in patients with LQTS compared with controls. **D:** Representative velocity-time diagram of 1 patient with LQTS with basal and apical longitudinal velocities. Note the longer basal TTP. **E:** Schematic and bull's-eye plots of longitudinal diastolic TTP in the base and apex (TTP_Vz_dia in ms) in healthy controls. **F:** Representative velocity-time diagram of 1 healthy control with basal and apical longitudinal velocities. Note the longer apical TTP.

In addition, we could confirm findings from a recently published study[9] demonstrating that patients with LQTS show a negative electromechanical window with QT duration pathologically outlasting contraction duration.

Dispersion of contraction duration in LQTS

Not only the prolongation of repolarization per se but also the regional dispersion of repolarization is known to play a major role in arrhythmogenesis in LQTS by providing a functional electrical substrate for reentry-based arrhythmia.[3] Despite this clear mechanistic relevance, the use of surface ECG markers indicative of increased regional and transmural dispersion of repolarization, such as QT dispersion and Tpeak-end dispersion, for risk stratification show conflicting results[21,22] and are hence not routinely used. Similarly, in our study, QT dispersion and Tpeak-end dispersion were not different in patients with LQTS and controls.

Because of close electromechanical coupling, the pronounced dispersion of repolarization should be reflected in a similarly pronounced mechanical dispersion. We thus hypothesize that distinct mechanical dispersion is present in patients with LQTS and can be detected with TPM MRI, allowing quantification of mechanical dispersion for all segments of the LV base, mid, and apex with a much higher spatial resolution than a more global assessment with surface ECG can provide. Through a comprehensive analysis of LV dispersion of contraction duration, we gained novel insights into altered mechanics in LQTS: We identified an increased apicobasal dispersion of contraction duration in longitudinal direction (with particularly prolonged contraction duration in the LV base) and an increased transmural and in-plane dispersion of contraction duration predominantly in the LV apex. The finding of prolonged contraction duration in the longitudinal direction is in line with a strain

echocardiography–based study by Haugaa et al,[14] reporting an increased transmural dispersion of contraction duration in the LV base due to prolongation of longitudinal contraction duration. Complementing these data, we provide first evidence that this prolongation of contraction duration is less pronounced in the LV apex (a region that has not previously been assessed by strain echocardiography). Therefore, longitudinal relaxation (eg, relaxation predominantly in line with the direction of endocardial "fiber sheets"[23]) in the LV base seems to be particularly affected by LQTS. Regarding mechanical dispersion in the LV apex, no data are available from other studies for comparison purposes, as most of the studies assessed myocardial contraction by strain echocardiography and did not measure radial or circumferential velocities in the LV apex. The pronounced segmental and transmural dispersion of contraction duration identified in the LV apex, however, suggests that the assessment of mechanical dysfunction with TPM MRI may add some important information on the extent of mechanical dysfunction in LQTS. Interestingly, these 2 regions with particularly an increased dispersion/prolongation of contraction duration—the longitudinal "endocardial fiber sheets" and the apex—correspond to the regions with the longest APD under physiological "normal" conditions.[24] Hence, one can speculate that in these regions electrical and mechanical function may be particularly affected by the malfunctioning of the mutated ion channels in LQTS.

Clinical implications

Bearing in mind that our study population with LQTS was young and mainly asymptomatic, we highlight the potential of TPM MRI to detect even subtle changes in magnitude and dispersion of myocardial mechanics. We suggest that analysis of myocardial mechanics and (subclinical) mechanical dysfunction might add additional information for arrhythmic risk stratification in the future.[9,10,12,13] Whether this mechanical dysfunction is causatively linked to increased arrhythmogenesis via direct mechanoelectrical coupling or (electromechanical) remodeling or whether regional mechanical dysfunction adds insights into risk mainly because it reflects regional electrical heterogeneities has yet to be determined. TPM MRI may be particularly useful to assess spatiotemporal mechanical dispersion as all LV regions and velocity directions may be analyzed.

Study limitations

The sympathetic nervous system affects both electrical and mechanical cardiac function. Thus, slight but nonsignificant heart rate differences and β-blocker therapy in patients with LQTS might have some confounding effect on contraction duration and dispersion of contraction duration. Further experiments are clearly indicated to elucidate the exact (nonlinear) relation of APD and contraction duration to establish an adequate heart rate correction formula for TTP_dia. Because of ethical reasons, we refrained from suspending β-blocker therapies for the duration of the study in patients, as it provides significant antiarrhythmic protection in LQTS and similarly did not initiate any nonindicated β-blocker therapy in healthy pediatric controls.

In this hypothesis-generating pilot study, mechanical function was assessed in a small number of young, mainly asymptomatic patients with LQTS. The findings on mechanical dispersion in LQTS thus clearly warrant confirmation in a larger multicenter study, including a more diverse patient population with LQTS to detect potential differences in the extent of mechanical dysfunction/dispersion at different ages, sexes, genotypes, and between symptomatic and asymptomatic patients to elucidate its potential use for future risk stratification.

Conclusion

In patients with LQTS, prolonged cardiac repolarization correlated with prolonged contraction duration, indicating an "electromechanical" disorder. Moreover, we identified a pronounced mechanical dispersion with an increased regional, base-apex, and transmural dispersion of contraction duration in LQTS. Importantly, we identified a partially reverse apicobasal sequence of relaxation in the longitudinal direction in LQTS. The detection of pronounced mechanical dispersion in LQTS using high-resolution TPM MRI despite the lack of detection of electrical dispersion using standard 12-lead ECG indicates that TPM MRI might add valuable information for risk stratification in LQTS in the future.

Appendix

Supplementary data

Supplementary data associated with this article can be found in the online version at http://dx.doi.org/10.1016/j.hrthm.2017.04.045.

References

1. Roden DM. Long-QT syndrome. N Engl J Med 2008;358:169–176.
2. Goldenberg I, Moss AJ. Long QT syndrome. J Am Coll Cardiol 2008;51:2291–2300.
3. Antzelevitch C. Role of spatial dispersion of repolarization in inherited and acquired sudden cardiac death syndromes. Am J Physiol Heart Circ Physiol 2008;148:825–832.
4. Pfeiffer ER, Tangney JR, Omens JH, McCulloch AD. Biomechanics of cardiac electromechanical coupling and mechanoelectric feedback. J Biomech Eng 2014;136:21007.
5. Quinn TA, Kohl P, Ravens U. Cardiac mechano-electric coupling research: fifty years of progress and scientific innovation. Prog Biophys Mol Biol 2014;115:71–75.
6. Nador F, Beria G, De Ferrari GM, Stramba-Badiale M, Locati EH, Lotto A, Schwartz PJ. Unsuspected echocardiographic abnormality in the long QT syndrome: diagnostic, prognostic, and pathogenetic implications. Circulation 1991;84:1530–1542.
7. De Ferrari GM, Nador F, Beria G, Sala S, Lotto A, Schwartz PJ. Effect of calcium channel block on the wall motion abnormality of the idiopathic long QT syndrome. Circulation 1994;89:2126–2132.
8. Savoye C, Klug D, Denjoy I, Ennezat PV, Le Tourneau T, Guicheney P, Kacet S. Tissue Doppler echocardiography in patients with long QT syndrome. Eur J Echocardiogr 2003;4:209–213.
9. Ter Bekke RMA, Haugaa KH, Van Den Wijngaard A, Bos JM, Ackerman MJ, Edvardsen T, Volders PGA. Electromechanical window negativity in genotyped long-QT syndrome patients: relation to arrhythmia risk. Eur Heart J 2015;36:179–186.
10. Lang CN, Menza M, Jochem S, et al. Electro-mechanical dysfunction in long QT syndrome: role for arrhythmogenic risk prediction and modulation by sex and sex hormones. Prog Biophys Mol Biol 2016;120:255–269.

11. Hummel YM, Wilde AA, Voors AA, Bugatti S, Hillege HL, van den Berg MP. Ventricular dysfunction in a family with long QT syndrome type 3. Europace 2013;15:1516–1521.
12. Nakayama K, Yamanari H, Otsuka F, Fukushima K, Saito H, Fujimoto Y, Emori T, Matsubara H, Uchida S, Ohe T. Dispersion of regional wall motion abnormality in patients with long QT syndrome. Heart 1998;80:245–250.
13. Haugaa KH, Edvardsen T, Leren TP, Gran JM, Smiseth OA, Amlie JP. Left ventricular mechanical dispersion by tissue Doppler imaging: a novel approach for identifying high-risk individuals with long QT syndrome. Eur Heart J 2009;30:330–337.
14. Haugaa KH, Amlie JP, Berge KE, Leren TP, Smiseth OA, Edvardsen T. Transmural differences in myocardial contraction in long-QT syndrome: mechanical consequences of ion channel dysfunction. Circulation 2010;122:1355–1363.
15. Leren IS, Hasselberg NE, Saberniak J, Håland TF, Kongsgård E, Smiseth OA, Edvardsen T, Haugaa KH. Cardiac mechanical alterations and genotype specific differences in subjects with long QT Syndrome. JACC Cardiovasc Imaging 2015;8:501–510.
16. Odening KE, Jung BA, Lang CN, et al. Spatial correlation of action potential duration and diastolic dysfunction in transgenic and drug-induced LQT2 rabbits. Heart Rhythm 2013;10:1533–1541.
17. Jung B, Foell D, Boettler P, Petersen S, Hennig J, Markl M. Detailed analysis of myocardial motion in volunteers and patients using high-temporal-resolution MR tissue phase mapping. J Magn Reson Imaging 2006;24:1033–1039.
18. Jung B, Odening KE, Dall'Armellina E, Föll D, Menza M, Markl M, Schneider JE. A quantitative comparison of regional myocardial motion in mice, rabbits and humans using in-vivo phase contrast CMR. J Cardiovasc Magn Reson 2012;14:87.
19. Vyas H, O'Leary PW, Earing MG, Cetta F, Ackerman MJ. Mechanical dysfunction in extreme QT prolongation. J Am Soc Echocardiogr 2008; 21:2007–2009.
20. Bassani RA. Transient outward potassium current and Ca^{2+} homeostasis in the heart: beyond the action potential. Braz J Med Biol Res 2006;39:393–403.
21. Malik M, Batchvarov VN. Measurement, interpretation and clinical potential of QT dispersion. J Am Coll Cardiol 2000;36:1749–1766.
22. Priori SG, Napolitano C, Diehl L, Schwartz PJ. Dispersion of the QT interval: a marker of therapeutic efficacy in the idiopathic long QT syndrome. Circulation 1994;89:1681–1689.
23. Lombaert H, Peyrat JM, Croisille P, Rapacchi S, Fanton L, Cheriet F, Clarysse P, Magnin I, Delingette H, Ayache N. Human atlas of the cardiac fiber architecture: study on a healthy population. IEEE Trans Med Imaging 2012;31:1436–1447.
24. Sengupta PP, Khandheria BK, Korinek J, Wang J, Jahangir A, Seward JB, Belohlavek M. Apex-to-base dispersion in regional timing of left ventricular shortening and lengthening. J Am Coll Cardiol 2006;47:163–172.